Published in final edited form as:
Eur J Nucl Med Mol Imaging. 2010 July ; 37(7): 1368–1376. doi:10.1007/s00259-009-1370-z.

PET imaging of HER1-expressing xenografts in mice with ^{86}Y-CHX-A"-DTPA-cetuximab

Tapan K. Nayak[1], **Celeste A.S. Regino**[1], **Karen J. Wong**[2], **Diane E. Milenic**[1], **Kayhan Garmestani**[1], **Kwamena E. Baidoo**[1], **Lawrence P. Szajek**[3], and **Martin W. Brechbiel**[1,*]

[1]Radioimmune & Inorganic Chemistry Section, Radiation Oncology Branch, National Cancer Institute, National Institutes of Health, Bethesda, MD, USA

[2]Molecular Imaging Program, National Cancer Institute, National Institute of Health, Bethesda, MD, USA

[3]PET Department, Warren G. Magnuson Clinical Center, National Institutes of Health, Bethesda, MD 20892-1180, USA

Abstract

Cetuximab is a recombinant, human/mouse chimeric IgG_1, monoclonal antibody (mAb) that binds to the epidermal growth factor receptor (EGFR/HER1). Cetuximab is approved for the treatment of patients with HER1-expressing metastatic colorectal cancer. Limitations in currently reported radiolabeled cetuximab for PET applications prompted the development of ^{86}Y-CHX-A"-DTPA-cetuximab as an alternative for imaging HER1-expressing cancer. ^{86}Y-CHX-A"-DTPA-cetuximab can also serve as a surrogate marker for ^{90}Y therapy.

Methods—Bifunctional chelate, CHX-A"-DTPA was conjugated to cetuximab and radiolabeled with ^{86}Y. *In vitro* immunoreactivity was assessed in HER1-expressing A431 cells. *In vivo* biodistribution, PET imaging and non-compartmental pharmacokinetics were performed on mice bearing HER1-expressing human colorectal (LS-174T and HT29), prostate (PC-3 and DU145), ovarian (SKOV3) and pancreatic (SHAW) tumor xenografts. Receptor blockage was demonstrated by co-injection of either 0.1 or 0.2 mg cetuximab.

Results—^{86}Y-CHX-A"-DTPA-cetuximab was routinely prepared with a specific activity of 1.5–2 GBq/mg and *in vitro* immunoreactivity ranging from 65–75 %. Biodistribution and PET imaging studies demonstrated high HER1-specific tumor uptake of the radiotracer and clearance from non-specific organs. In LS-174T tumor bearing mice injected with the ^{86}Y-CHX-A"-DTPA-cetuximab alone, ^{86}Y-CHX-A"-DTPA-cetuximab plus 0.1 mg cetuximab or 0.2 mg cetuximab, the tumor uptake values at 3 d were 29.3 ± 4.2, 10.4 ± 0.5 and 6.4 ± 0.3 % ID/g, respectively, demonstrating dose-dependent blockage of the target. Tumors were clearly visualized 1 d after injecting 3.8–4.0 MBq ^{86}Y-CHX-A"-DTPA-cetuximab. Quantitative PET revealed highest tumor uptake in LS-174T (29.55 ± 2.67 % ID/cc) and lowest tumor uptake in PC-3 (15.92 ± 1.55 % ID/cc) xenografts at 3 d after injection. Tumor uptake values quantified by PET were closely correlated (r^2= 0.9, n=18) to values determined by biodistribution studies.

Conclusion—This study demonstrates the feasibility in preparation of high specific activity ^{86}Y-CHX-A"-DTPA-cetuximab and its application for quantitative non-invasive PET imaging of HER1-

[*]**Corresponding author and reprint requests**: Dr. Martin W. Brechbiel, 10 Center Drive MSC-1002, Building 10, Room B3B69, Bethesda, Bethesda, MD 20892. Fax: 301-402-1923. martinwb@mail.nih.gov. **First author (Post-doctoral fellow)**: Tapan K. Nayak, 10 Center Drive MSC-1002, Building 10, Room B3B69, Bethesda, Bethesda, MD 20892. tapann@gmail.com.

Authors declare no conflict of interests.

expressing tumors. ^{86}Y-CHX-A"-DTPA-cetuximab offers an attractive alternative to previously labeled cetuximab for PET and warrants further investigation for clinical translation.

Keywords

PET imaging; HER1; Cetuximab; Radioimmunoimaging; ^{86}Y

Introduction

Targeted therapy is becoming increasingly utilized in the armamentarium in the fight to treat cancer. Among the targets under active investigation for the development of effective targeted therapies, the epidermal growth factor receptor (EGFR/HER1) has shown great promise. The receptor plays an important role in tumorigenesis by controlling the signaling pathways that regulate proliferation, survival, angiogenesis, invasion and metastasis [1,2]. Cetuximab (IMC-225, Erbitux®), a recombinant, human/mouse chimeric immunoglobulin G_1 monoclonal antibody (mAb), binds specifically to the extracellular domain of the human HER1 [1–3]. Cetuximab inhibits binding of the endogenous ligands, EGF and TGF-α, to the receptor causing receptor internalization without stimulating receptor phosphorylation, thereby preventing ligand-mediated receptor tyrosine kinase phosphorylation [1,2]. Cetuximab exerts antitumor effects by inhibition of cell cycle progression, promotion of apoptosis, anti-angiogenesis and antibody-dependent cellular cytotoxicity [1–3]. Cetuximab, as approved by the FDA in 2004, has been indicated for the treatment of patients with metastatic colorectal cancer whose tumors are positive for EGFR either in combination with irinotecan, or alone if patients cannot tolerate irinotecan [4]. Cetuximab gained the approval under the U.S. FDA's accelerated approval program, which allows FDA to approve products for cancer and other serious or life-threatening diseases based on early evidence of a product's effectiveness [1]. In addition to colorectal cancer, cetuximab is under clinical investigation for treatment of head and neck cancer, non-small cell lung cancer and advanced breast cancer.

Techniques such as immunohistochemistry (IHC), gene copy number by fluorescent in situ hybridization (FISH), and mutation analysis by sequencing are currently used to screen patients for cetuximab related therapy [5,6]. Along with traditional pathological procedures and tests such as biopsies, non-invasive nuclear imaging is often used to assess the status of the specific target. To assess the status of HER1-expression and cetuximab distribution, cetuximab has previously been labeled with radionuclides such as ^{99m}Tc and ^{111}In for single photon emission computerized tomography (SPECT) imaging [7–10] as well as ^{64}Cu and ^{89}Zr for positron emission tomography (PET) [11–15]. Cetuximab labeled with ^{64}Cu and ^{89}Zr exhibited several disadvantages in these studies due to the lack of stable chelating agents and simple radiosynthesis procedures. ^{64}Cu-DOTA-cetuximab had relatively poor tumor-to-blood and tumor-to-background ratios due to dissociation of ^{64}Cu from the DOTA complex [11–13]. Increased liver uptake was also evident with ^{64}Cu-DOTA-cetuximab, which may limit its application in imaging liver metastasis in advanced colorectal cancer. In order to minimize dissociation of ^{64}Cu from DOTA, cross-bridged tetraamine chelating agents have been proposed [16,17]. However, these agents require heating, up to 95° C, for successful incorporation of ^{64}Cu and therefore may not be appropriate for proteins such as cetuximab. The biggest disadvantage for ^{89}Zr labeled cetuximab is the tedious multi-step radiosynthesis procedure. Furthermore, accumulation of ^{89}Zr in the bone has been observed, a result of leakage of this radioisotope from desferoxamine (Df) [14,18]. To curtail the problems associated with ^{64}Cu and ^{89}Zr and as an alternative for a cetuximab targeted PET agent, the preparation and preclinical evaluation of cetuximab conjugated with CHX-A"-DTPA and radiolabeled with ^{86}Y for PET is described herein. ^{86}Y was selected due to its appropriate half-life of 14.7 h, suitability for internalizing mAbs, well-established chelation chemistry, and reasonable availability [18,19]. In addition to these attractive features, ^{86}Y can also serve as a surrogate

PET marker for ^{90}Y- CHX-A"-DTPA-cetuximab radioimmunotherapy (RIT) of solid tumors [20]. The primary objective of this study is the pre-clinical evaluation of the anti-HER1 antibody cetuximab, labeled with the positron emitting nuclide ^{86}Y, for imaging access of the antibody to the receptor in HER1-expressing tumors.

Methods and materials

Preparation of ^{86}Y-CHX-A"-DTPA-cetuximab

Radiolabeling CHX-A"-DTPA-cetuximab with ^{86}Y—The bifunctional chelate, CHX-A"-DTPA, was conjugated to cetuximab as previously described [10]. The chelate to protein ratio was spectrophotometrically determined using the Y(III)-Arsenazo(III) complex assay [10,21]. ^{86}Y was produced through the ^{86}Sr(p,n)^{86}Y reaction as previously described [19].

For radiolabeling, a freshly prepared solution of ascorbic acid (50 μL, 220 μg/ μL) was first added to the ^{86}Y solution (140–170 MBq in 0.1 M nitric acid, 500 μL) to prevent radiolysis. The ^{86}Y solution was then neutralized to pH 5 – 6 by the addition of an ammonium acetate buffer (50 μL, 5 M, pH 7.0). CHX-A"-DTPA-cetuximab (50 μg in 0.15 M ammonium acetate) was added to the mixture, vortexed briefly, and then incubated at room temperature for 30 min. The reaction was quenched by the addition of 0.1 M EDTA (4 μL). The radiolabeled product was purified using a PD-10 desalting column (GE Healthcare, Piscataway, NJ, USA). Size exclusion HPLC (SE-HPLC) chromatography using a TSK-3000 column (Toso-Haas, Montgomeryville, PA, USA) was performed to ascertain the purity of the radioimmunoconjugate as previously described [19].

Cell culture

HER1-expressing human colorectal (LS-174T and HT29), prostate (PC-3 and DU145), ovarian (SKOV3), pancreatic (SHAW) and epidermoid (A431) carcinoma cells (American Type Culture Collection, Rockville, MD, USA) were grown as monolayers at 37° C, in a humidified atmosphere of 5% CO_2 and 95% air as previously described [10]. Media and supplements were obtained from Quality Biologicals (Gaithersburg, MD, USA), Invitrogen (Carlsbad, CA, USA) and Lonza (Walkersville, MD, USA).

In vitro evaluation

Radioligand cell-binding studies—The immunoreactivity of the ^{86}Y-CHX-A"-DTPA-cetuximab was determined using a fixed-cell radioimmunoassay (RIA) as previously described [10].

Animal and tumor models

Groups of 5–8 week old female athymic *nu/nu* mice (Charles River Laboratory, Wilmington, MA USA) were injected subcutaneously with 2×10^6 cells of each cell line (200 μL medium containing 20% matrigel).

In vivo evaluations

Biodistribution and pharmacokinetic studies—Tumor bearing female athymic mice were intravenously (i.v.) injected with 0.4–0.6 MBq (< 5 μg) of ^{86}Y-CHX-A"-DTPA-cetuximab. To determine HER1-specificity, cetuximab (0.1 and 0.2 mg) was co-injected with the radiotracer in an additional set of mice bearing each of the tumor xenografts. A dose escalation study (0.4–0.6 MBq/ 5–200 μg) was performed to determine the effects of mass injected and saturation of the target using LS-174T tumor bearing mice. At the desired time points, the animals were sacrificed by CO_2 inhalation. Tumor, blood and selected organs were harvested, wet-weighed, and the radioactivity was measured in a Wallac Wizard 1480 gamma

counter (PerkinElmer, Shelton, CT). The percent injected dose per gram (% ID/g) of tissue was calculated by comparison with standards representing 10% of the injected dose per animal. Non-compartmental pharmacokinetics was performed to determine area under the curve (AUC), area under the moment curve (AUMC) and the mean residence time (MRT) using trapezoidal integration analysis [22].

PET imaging studies—Small animal PET studies were performed using the ATLAS (Advanced Technology Laboratory Animal Scanner) at the National Institutes of Health, Bethesda, MD, USA [23]. Whole body imaging studies (6 bed positions, total acquisition time of 1 h per mouse) were carried out on mice anesthetized with 1.5–1.7% isoflurane on a temperature-controlled bed. Tumor bearing female athymic mice were injected i.v. with 3.8–4.0 MBq (< 5 μg) of ^{86}Y-CHX-A”-DTPA-cetuximab. To determine HER1-specificity, excess cetuximab (0.1 and 0.2 mg) was co-injected with the radiotracer. ^{86}Y cylinder phantoms were imaged each day for normalization and quantitative analysis. The energy window for PET acquisition of ^{86}Y was set between 400 and 700 keV. The imaging data were reconstructed using Fourier Rebinned - Ordered Subsets Expectation Maximization method with scatter correction (linear background subtraction). Additional dead time, partial volume, scatter, decay and background corrections were applied for quantitative analysis. The reconstructed images were processed and analyzed using AMIDE (A Medical Image Data Examiner) software program. To minimize spillover effects, regions of interest (ROIs) were drawn to enclose approximately 80–90% of the organ of interest in order to avoid the edges. To minimize partial-volume effects caused by non-uniform distribution of the radioactivity in the containing volume, smaller ROIs were consistently drawn to enclose the organ. After imaging, the mice were euthanized and biodistribution studies were performed to determine the correlation between PET-assessed *in vivo* % ID/cc and biodistribution determined % ID/g. The animal studies were performed in accordance with the NIH guidelines for the humane use of animals and all procedures were reviewed and approved by the National Cancer Institute Animal Care and Use Committee.

Statistical Analysis

All numerical data were expressed as the mean of the values ± the standard error of mean (SEM). Graphpad Prism version 5 (San Diego, CA, USA) was used for statistical analysis. A *p* value less than 0.05 was considered statistically significant.

Results

Radiochemistry and *In vitro* evaluations

Modification of cetuximab with the acyclic ligand CHX-A”-DTPA was performed at a 10:1 molar excess of chelate to protein yielding a final chelate to protein ratio of 2.3. Studies from this laboratory have previously demonstrated that conjugating 2–3 molecules of CHX-A”-DTPA to cetuximab did not alter the immunoreactivity of cetuximab [10]. The ^{86}Y-CHX-A”-DTPA-cetuximab conjugate was successfully prepared with radiochemical yields ranging from 55–75% and a specific activity up to 1.5–2 GBq/mg. The absolute immunoreactivity of ^{86}Y-CHX-A”-DTPA-cetuximab based on the cell binding assay ranged from 65–75% demonstrating *in vitro* specificity. The non-specific binding determined from blocking experiments was less than 4%. On HPLC analysis, the RIC exhibited excellent stability and retained immunoreactivity and the expected HPLC profile (Supplemental Figure 1) after storage at 4° C for up to 1 d.

In vivo evaluations

Biodistribution studies—In mice bearing LS-174T tumor xenografts, approximately 70% decrease in the blood pool activity was observed over a 4 d time period (14.09 ± 1.31 % ID/g

at 1 d to 4.03 ± 0.52 % ID/g at 4 d) (Fig 1A). Similarly, a 60% decrease was observed in liver uptake over a 4 d time period (10.77± 1.24 % ID/g at 1 d to 4.91 ± 1.14 % ID/g at 4 d). In contrast, an approximate 30% increase was observed in tumor uptake, with the % ID/g of 21.23 ± 1.00 at 1 d increasing to 27.42 ± 3.59 at 4 d after injection (Fig. 1A). The tumor-to-blood ratio increased 4.5-fold from 1.5 at 1 d to 6.8 at 4 d after injection. The ^{86}Y-CHX-A"-DTPA-cetuximab uptake in tumor was dose-dependent and HER1-mediated as demonstrated by the receptor-blocking experiments performed by co-injecting 0.1 mg and 0.2 mg cetuximab (Fig 1B). The LS-174T tumor uptake of 29.31 ± 4.20 % ID/g at 3 d after injection was significantly greater than mice co-injected with either 0.1 mg cetuximab (10.41 ± 0.47 % ID/g at 3 d, p = 0.012) or 0.2 mg cetuximab (6.37 ± 0.29 % ID/g at 3 d, p = 0.005). The blocking by 0.1 mg and 0.2 mg cetuximab were significantly different (p = 0.001) indicative of a dose-dependent saturation of HER1 in the tumor xenografts. Dose escalation studies revealed significant decrease in tumor uptake when the injected mass was more than 10 μg (Suppl. Fig 2).

PET imaging studies and pharmacokinetic analysis—The linearity of the PET-assessed concentration *vs*. the radioactivity concentration measured in a Capintec CRC-127R dose calibrator was r^2= 0.99 in the range of 0.03–3.63 MBq/mL of ^{86}Y solution determined by cylindrical phantom studies.

PET imaging studies were performed with female athymic mice bearing LS-174T (Fig. 2A–C), SHAW (Fig. 3A), HT29 (Fig. 3B), DU145 (Fig. 3C), SKOV3 (Fig. 3D) and PC-3 tumors (not shown) injected with 3.8–4.0 MBq of ^{86}Y-CHX-A"-DTPA-cetuximab. Blocking studies were performed on mice bearing LS-174T tumor by co-injecting 0.1 mg cetuximab (Fig. 2B) and 0.2 mg cetuximab (Fig. 2C). All of the tumors were clearly visualized from 1 to 3 d after injection of the RIC as shown in maximum intensity projection images (Fig. 2 and 3). The tumor-to-background ratios improved over this period mostly as the radioactivity in the blood and liver decreased while the tumor uptake continued to increase. Quantitative PET revealed the highest tumor uptake in the LS-174T tumors (29.55 ± 2.67 % ID/cc) while the PC3 xenografts presented with the lowest tumor uptake (15.92 ± 1.55 % ID/cc) 3 d after injection of the ^{86}Y-CHX-A"-DTPA-cetuximab (Fig. 4). In contrast, when 0.1 mg of cetuximab was co-injected with the radiotracer, the tumors were poorly visualized, demonstrating the HER1-specificity of ^{86}Y-CHX-A"-DTPA-cetuximab (Fig. 2B and Fig. 4). Further blockage was observed when 0.2 mg of ceuximab was co-injected (Fig. 2C and Fig. 4). As shown in Fig. 4, the quantified tumor uptake of mice injected with ^{86}Y-CHX-A"-DTPA-cetuximab and mice co-injected with 0.1 mg and 0.2 mg excess cetuximab were significantly different at 1 d, 2 d and 3 d post-injection. For mice bearing LS-174T tumors, the PET assessed tumor $AUC_{[0\rightarrow3]}$ and $AUMC_{[0\rightarrow3]}$ of mice injected with ^{86}Y-CHX-A"-DTPA-cetixumab was 2.3 and 4.1 times greater than that of mice co-injected with 0.1 mg and 0.2 mg cetuximab, respectively (Table 1). Mice bearing PC-3 tumors demonstrated the lowest tumor $AUC_{[0\rightarrow3]}$ and $AUMC_{[0\rightarrow3]}$ (Table 1). However, all of the tumor xenograft models were found to have had identical mean tumor residence times (MRT) of 2.1–2.5 d. The tumor uptake values quantified by PET were closely correlated (r^2= 0.9, n = 18) to the values determined by *ex vivo* biodistribution studies at 1, 2 and 3 d after injection.

Discussion

In the past few decades, targeted noninvasive nuclear imaging has been used to study key biochemical and physiological processes. In addition to target occupancy and disease staging, noninvasive nuclear imaging can be used to determine pharmacokinetics and pharmacodynamics without significantly disrupting the underlying biochemical and physiological process under study [24]. Towards this end, ^{64}Cu and ^{89}Zr labeled cetuximab were developed to stage HER1-expressing cancer, and to determine the pharmacokinetics of cetuximab [11–15]. HER1-expressing tumors were successfully imaged with both, ^{64}Cu

and ^{89}Zr labeled cetuximab. However, in the case of ^{64}Cu labeled cetuximab, the liver uptake at 2 d after injection (~15 %ID/g) was over 50 % greater than that of ^{86}Y-CHX-A"-DTPA-cetuximab (~ 10 % ID/g) [12]. We found a steady decrease in liver uptake from 10.75 ± 1.24 % ID/g at 1 d after injection to 4.91± 1.24 % ID/g at 4 d after injection. In contrast, the liver uptake increased over this period for ^{64}Cu labeled cetuximab indicative of metabolism due to challenging chelation chemistry. ^{64}Cu-TETA-1A3 has previously been reported for clinical PET imaging of metastatic colorectal cancer [25,26]. Although all 17 primary and recurrent sites were clearly visualized in patients, only 23 of 39 metastatic sites (59 %) were detected [26]. Detection of lung and liver metastases were seriously hindered by accumulation of radioactivity in the liver and the blood due to dissociation of the ^{64}Cu from the currently used chelates for radiolabeling mAbs. While the half-life of ^{86}Y is slightly longer than ^{64}Cu, the abundance of positrons is also almost twice that of ^{64}Cu. With these advantages over ^{64}Cu, much lower amounts of injected ^{86}Y will be required for quantitative immunoPET after 2 d post injection. Based on previous studies performed with ^{64}Cu labeled mAb [25,26], 0.18–0.37 GBq of the ^{86}Y-labeled RIC should result in useful quantitative images up to 2–3 d post-injection. ^{89}Zr labeled mAbs were proposed as surrogate PET markers for dosimetry of ^{90}Y labeled mAbs, however, ^{89}Zr labeled cetuximab had almost twice the level of bone uptake than ^{88}Y labeled cetuximab [14]. Therefore, ^{86}Y labeled cetuximab might be a better surrogate PET marker than ^{89}Zr labeled cetuximab for dosimetry of ^{90}Y labeled cetuximab. Furthermore, the preparation of ^{89}Zr labeled cetuximab is tedious, time-consuming and involves over 7 steps with a total preparation time of over 3 hours [14]. However, the recently reported bifunctional chelate, *p*-isothiocyanatobenzyl-desferrioxamine provides an alternative for facile radiolabeling of monoclonal antibodies with ^{89}Zr [27]. The preparation of high specific activity ^{86}Y-CHX-A"-DTPA-cetuximab reported in this study is straightforward with direct incorporation of ^{86}Y to the CHX-A"-DTPA-cetuximab at room temperature in less than an hour.

Previous clinical studies with ^{111}In labeled 225 (murine version of cetuximab) suggest that the optimal injected dose of radiolabeled cetuximab for optimum target to background ratio should be about 120 mg [28]. Therefore, it is anticipated that the specific activity of ^{86}Y-CHX-A"-DTPA-cetuximab needed for clinical studies will be considerably lower than reported in this preclinical study. However, for animal studies, high specific activity is required to avoid saturation of the target (Suppl. Fig. 2) illustrating the limitations of animal studies to predict the specific activity required for clinical studies. The same study also reported the presence of HER1 receptor in the liver based on the dose-dependent liver uptake and clearance of the ^{111}In labeled murine 225. However, studies performed with radiolabeled chimeric mAb, C225 (cetuximab) concluded that the residence time in the liver appeared to be longer in patients with cold loading than in those without [8]. One explanation could indeed be that the liver does not have C225 binding sites, but simply metabolically extracts whatever is not taken up elsewhere in the body. In the preclinical study performed in the report, the uptake in liver was not blocked by co-injecting excess cetuximab, suggesting the lack of cetuximab binding sites in mice liver, which concurs with the information provided by the manufacturer of cetuximab, ImClone Systems [29].

In spite of the advantages of ^{86}Y labeled cetuximab over ^{64}Cu and ^{89}Zr, ^{86}Y has its own set of limitations. Yttrium-86 has, in fact, a high positron energy (E_{max} = 3.1 MeV) with an additional γ-emission of 1.08 MeV (83% abundance) which can significantly affect the image quality and recovery coefficients due to spurious coincidences [18]. When appropriate corrections are performed, however, the image quality is greatly improved and is quantifiable as shown in this study as well as by others [30,31]. In this study, normalization experiments were performed with a cylinder phantom filled with ^{86}Y solution during each imaging session to apply appropriate corrections. After the partial volume, scatter and background corrections,

the tumor uptake quantified by PET was closely related (r^2= 0.9, n = 18) to values determined by *ex vivo* biodistribution studies at 1, 2 and 3 d after injection.

PET imaging with ^{86}Y-CHX-A”-DTPA-cetuximab may have a useful role in patient selection for cetuximab related therapy since it would indicate HER1 accessibility to the antibody. However, ^{86}Y-CHX-A”-DTPA-cetuximab imaging by itself may not predict the response to therapy as it is only indicative of how much cetuximab reaches the tumor and not the overall tumor HER1 expression, microenvironment and the biomolecular characteristics. It does not provide any information regarding the status of KRAS mutations and loss of PTEN, which is critical for response to HER1 immunotherapy [6,32–34]. Therefore, PET imaging with radiolabeled cetuximab may be complimentary and used together with assays to determine KRAS mutations, loss of PTEN and HER1 gene amplification and polymorphism [32–34].

The potential of ^{90}Y-CHX-A”-DTPA-cetuximab for radioimmunotherapy is currently under evaluation in this laboratory utilizing the LS-174T tumor model. Cetuximab radiolabeled with ^{86}Y would serve as a means of monitoring responsiveness to the therapy and provide dosimetry data. Ultimately, ^{86}Y-CHXA”-DTPA-cetuximab would be a surrogate PET marker for dosimetry and selection of subjects for ^{90}Y CHX-A”-DTPA-cetuximab RIT of HER1-expressing cancers. As discussed, the primary objective of this study was to develop a PET tracer to assess cetuximab biodistribution and pharmacokinetic characteristics. For HER1 imaging, other targeting modalities such as radiolabeled affibodies, nanobodies, tyrosine kinase inhibitors and EGF have also been successfully used [35–38].

To achieve the long-term goal of clinical translation of ^{86}Y-CHX-A”-DTPA-cetuximab, PET/CT and MRI studies are currently being performed with mice bearing orthotopic and disseminated tumors.

Conclusion

In conclusion, the utility of ^{86}Y-CHX-A”-DTPA-cetuximab for non-invasive PET imaging of HER1-expressing tumors in preclinical models has been demonstrated. ^{86}Y-CHX-A”-DTPA-cetuximab is a viable alternative to ^{64}Cu and ^{89}Zr labeled cetuximab due to lower liver uptake, better tumor to blood and background ratios as well as ease of preparation. ^{86}Y-CHX-A”-DTPA-cetuximab may be useful for the assessment of cetuximab uptake, which may be important for risk stratification, patient screening and appropriate dosage selection.

Supplementary Material

Refer to Web version on PubMed Central for supplementary material.

Acknowledgments

This research was supported by the Intramural Research Program of the National Institute of Health, National Cancer Institute, Center for Cancer Research and the United States Department of Health and Human Services. Gratitude is expressed to Jurgen Seidel and Michael Green (National Cancer Institute, National Institute of Health, Bethesda, MD) for technical input on the operations of NIH ATLAS small animal PET scanner.

Financial support: The Intramural Research Program of the NIH, NCI, Center for Cancer Research and the United States Department of Health and Human Services.

References

1. Mendelsohn J, Baselga J. Epidermal growth factor receptor targeting in cancer. Semin Oncol 2006;33:369–85. [PubMed: 16890793]

2. Harari PM. Epidermal growth factor receptor inhibition strategies in oncology. Endocr Relat Cancer 2004;11:689–708. [PubMed: 15613446]
3. Capdevila J, Elez E, Macarulla T, Ramos FJ, Ruiz-Echarri M, Tabernero J. Anti-epidermal growth factor receptor monoclonal antibodies in cancer treatment. Cancer Treat Rev 2009;35:354–63. [PubMed: 19269105]
4. Cunningham D, Humblet Y, Siena S, Khayat D, Bleiberg H, Santoro A, et al. Cetuximab monotherapy and cetuximab plus irinotecan in irinotecan-refractory metastatic colorectal cancer. N Engl J Med 2004;351:337–45. [PubMed: 15269313]
5. Personeni N, Fieuws S, Piessevaux H, De Hertogh G, De Schutter J, Biesmans B, et al. Clinical usefulness of EGFR gene copy number as a predictive marker in colorectal cancer patients treated with cetuximab: a fluorescent in situ hybridization study. Clin Cancer Res 2008;14:5869–76. [PubMed: 18794099]
6. Loupakis F, Pollina L, Stasi I, Ruzzo A, Scartozzi M, Santini D, et al. PTEN expression and KRAS mutations on primary tumors and metastases in the prediction of benefit from cetuximab plus irinotecan for patients with metastatic colorectal cancer. J Clin Oncol 2009;27:2622–9. [PubMed: 19398573]
7. Wen X, Wu QP, Ke S, Ellis L, Charnsangavej C, Delpassand AS, et al. Conjugation with (111)In-DTPA-poly(ethylene glycol) improves imaging of anti-EGF receptor antibody C225. J Nucl Med 2001;42:1530–7. [PubMed: 11585869]
8. Schechter NR, Wendt RE 3rd, Yang DJ, Azhdarinia A, Erwin WD, Stachowiak AM, et al. Radiation dosimetry of 99mTc-labeled C225 in patients with squamous cell carcinoma of the head and neck. J Nucl Med 2004;45:1683–7. [PubMed: 15471833]
9. Barrett T, Koyama Y, Hama Y, Ravizzini G, Shin IS, Jang BS, et al. In vivo diagnosis of epidermal growth factor receptor expression using molecular imaging with a cocktail of optically labeled monoclonal antibodies. Clin Cancer Res 2007;13:6639–48. [PubMed: 17982120]
10. Milenic DE, Wong KJ, Baidoo KE, Ray GL, Garmestani K, Williams M, et al. Cetuximab: preclinical evaluation of a monoclonal antibody targeting EGFR for radioimmunodiagnostic and radioimmunotherapeutic applications. Cancer Biother Radiopharm 2008;23:619–31. [PubMed: 18999934]
11. Ping Li W, Meyer LA, Capretto DA, Sherman CD, Anderson CJ. Receptor-binding, biodistribution, and metabolism studies of 64Cu-DOTA-cetuximab, a PET-imaging agent for epidermal growth-factor receptor-positive tumors. Cancer Biother Radiopharm 2008;23:158–71. [PubMed: 18454685]
12. Cai W, Chen K, He L, Cao Q, Koong A, Chen X. Quantitative PET of EGFR expression in xenograft-bearing mice using 64Cu-labeled cetuximab, a chimeric anti-EGFR monoclonal antibody. Eur J Nucl Med Mol Imaging 2007;34:850–8. [PubMed: 17262214]
13. Eiblmaier M, Meyer LA, Watson MA, Fracasso PM, Pike LJ, Anderson CJ. Correlating EGFR expression with receptor-binding properties and internalization of 64Cu-DOTA-cetuximab in 5 cervical cancer cell lines. J Nucl Med 2008;49:1472–9. [PubMed: 18703609]
14. Perk LR, Visser GW, Vosjan MJ, Stigter-van Walsum M, Tijink BM, Leemans CR, et al. (89)Zr as a PET surrogate radioisotope for scouting biodistribution of the therapeutic radiometals (90)Y and (177)Lu in tumor-bearing nude mice after coupling to the internalizing antibody cetuximab. J Nucl Med 2005;46:1898–906. [PubMed: 16269605]
15. Aerts HJ, Dubois L, Perk L, Vermaelen P, van Dongen GA, Wouters BG, et al. Disparity between in vivo EGFR expression and 89Zr-labeled cetuximab uptake assessed with PET. J Nucl Med 2009;50:123–31. [PubMed: 19091906]
16. Boswell CA, Regino CA, Baidoo KE, Wong KJ, Bumb A, Xu H, et al. Synthesis of a cross-bridged cyclam derivative for peptide conjugation and 64Cu radiolabeling. Bioconjug Chem 2008;19:1476–84. [PubMed: 18597510]
17. Boswell CA, Sun X, Niu W, Weisman GR, Wong EH, Rheingold AL, et al. Comparative in vivo stability of copper-64-labeled cross-bridged and conventional tetraazamacrocyclic complexes. J Med Chem 2004;47:1465–74. [PubMed: 14998334]
18. Nayak TK, Brechbiel MW. Radioimmunoimaging with Longer-Lived Positron-Emitting Radionuclides: Potentials and Challenges. Bioconjug Chem 2009;20:825–41. [PubMed: 19125647]

19. Garmestani K, Milenic DE, Plascjak PS, Brechbiel MW. A new and convenient method for purification of 86Y using a Sr(II) selective resin and comparison of biodistribution of 86Y and 111In labeled Herceptin. Nucl Med Biol 2002;29:599–606. [PubMed: 12088731]
20. Palm S, Enmon RM Jr. Matei C, Kolbert KS, Xu S, Zanzonico PB, et al. Pharmacokinetics and Biodistribution of (86)Y-Trastuzumab for (90)Y dosimetry in an ovarian carcinoma model: correlative MicroPET and MRI. J Nucl Med 2003;44:1148–55. [PubMed: 12843231]
21. Pippin CG, Parker TA, McMurry TJ, Brechbiel MW. Spectrophotometric method for the determination of a bifunctional DTPA ligand in DTPA-monoclonal antibody conjugates. Bioconjug Chem 1992;3:342–5. [PubMed: 1390990]
22. Gibaldi, M.; Perrier, D. Pharmacokinetics. 2nd ed.. Dekker; New York: 1982.
23. Seidel J, Vaquero JJ, Green MV. Resolution Uniformity and Sensitivity of the NIH ATLAS Small Animal PET Scanner: Comparison to Simulated LSO Scanners Without Depth-of-Interaction Capability. IEEE Transactions on Nuclear Science 2003;50:1347–50.
24. Eckelman WC, Reba RC, Kelloff GJ. Targeted imaging: an important biomarker for understanding disease progression in the era of personalized medicine. Drug Discov Today 2008;13:748–59. [PubMed: 18617011]
25. Cutler PD, Schwarz SW, Anderson CJ, Connett JM, Welch MJ, Philpott GW, et al. Dosimetry of copper-64-labeled monoclonal antibody 1A3 as determined by PET imaging of the torso. J Nucl Med 1995;36:2363–71. [PubMed: 8523133]
26. Philpott GW, Schwarz SW, Anderson CJ, Dehdashti F, Connett JM, Zinn KR, et al. RadioimmunoPET: detection of colorectal carcinoma with positron-emitting copper-64-labeled monoclonal antibody. J Nucl Med 1995;36:1818–24. [PubMed: 7562049]
27. Perk LR, Vosjan MJ, Visser GW, Budde M, Jurek P, Kiefer GE, et al. p-Isothiocyanatobenzyl-desferrioxamine: a new bifunctional chelate for facile radiolabeling of monoclonal antibodies with zirconium-89 for immuno-PET imaging. Eur J Nucl Med Mol Imaging. 2009 10.1007/s00259-009-1263-1 10.1007/s00259-009-1263-1.
28. Divgi CR, Welt S, Kris M, Real FX, Yeh SD, Gralla R, et al. Phase I and imaging trial of indium 111-labeled anti-epidermal growth factor receptor monoclonal antibody 225 in patients with squamous cell lung carcinoma. J Natl Cancer Inst 1991;83:97–104. [PubMed: 1988695]
29. ImClone. ImClone Systems Incorporated. Cetuximab: Epidermal Growth Factor Receptor (EGFR) Antibody. Version 9.0. ImClone Systems, Inc.; New York: 2003.
30. Liu X, Laforest R. Quantitative small animal PET imaging with nonconventional nuclides. Nucl Med Biol 2009;36:551–9. [PubMed: 19520296]
31. Herzog H, Tellmann L, Scholten B, Coenen HH, Qaim SM. PET imaging problems with the non-standard positron emitters Yttrium-86 and Iodine-124. Q J Nucl Med Mol Imaging 2008;52:159–65. [PubMed: 18043538]
32. Di Nicolantonio F, Martini M, Molinari F, Sartore-Bianchi A, Arena S, Saletti P, et al. Wild-Type BRAF Is Required for Response to Panitumumab or Cetuximab in Metastatic Colorectal Cancer. J Clin Oncol 2008;26:5705–5712. [PubMed: 19001320]
33. Amado RG, Wolf M, Peeters M, Van Cutsem E, Siena S, Freeman DJ, et al. Wild-type KRAS is required for panitumumab efficacy in patients with metastatic colorectal cancer. J Clin Oncol 2008;26:1626–34. [PubMed: 18316791]
34. Jimeno A, Messersmith WA, Hirsch FR, Franklin WA, Eckhardt SG. KRAS mutations and sensitivity to epidermal growth factor receptor inhibitors in colorectal cancer: practical application of patient selection. J Clin Oncol 2009;27:1130–6. [PubMed: 19124802]
35. Tolmachev V, Rosik D, Wallberg H, Sjoberg A, Sandstrom M, Hansson M, et al. Imaging of EGFR expression in murine xenografts using site-specifically labelled anti-EGFR (111)In-DOTA-Z (EGFR:2377) Affibody molecule: aspect of the injected tracer amount. Eur J Nucl Med Mol Imaging. 2009 10.1007/s00259-009-1283-x 10.1007/s00259-009-1283-x.
36. Gainkam LO, Huang L, Caveliers V, Keyaerts M, Hernot S, Vaneycken I, et al. Comparison of the biodistribution and tumor targeting of two 99mTc-labeled anti-EGFR nanobodies in mice, using pinhole SPECT/micro-CT. J Nucl Med 2008;49:788–95. [PubMed: 18413403]
37. Mishani E, Hagooly A. Strategies for molecular imaging of epidermal growth factor receptor tyrosine kinase in cancer. J Nucl Med 2009;50:1199–202. [PubMed: 19617320]

38. Mishani E, Abourbeh G, Eiblmaier M, Anderson CJ. Imaging of EGFR and EGFR tyrosine kinase overexpression in tumors by nuclear medicine modalities. Curr Pharm Des 2008;14:2983–98. [PubMed: 18991714]

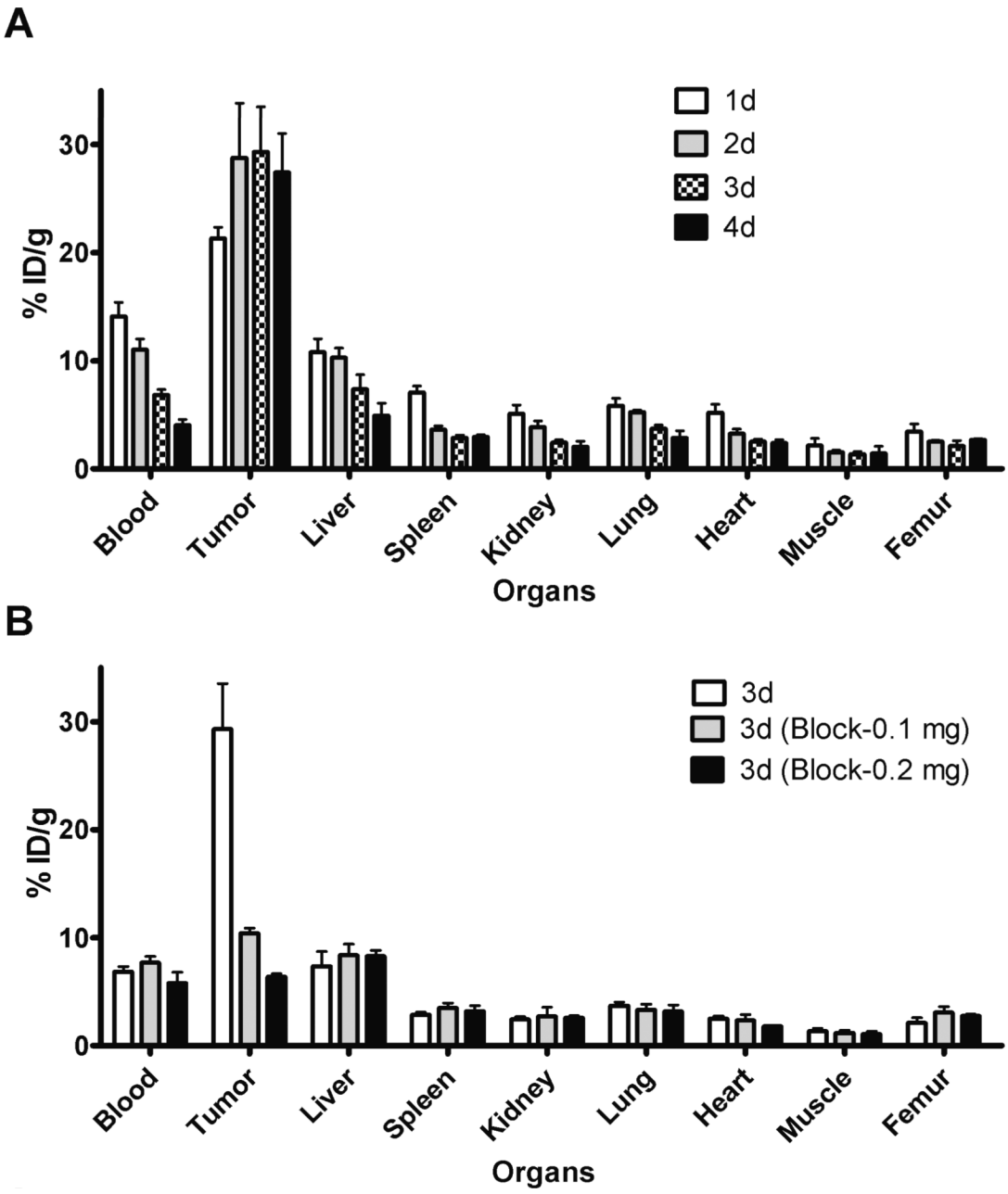

Figure 1.

(A) Biodistribution of ^{86}Y-CHX-A"-DTPA-cetuximab in selected organs of female athymic (NCr) *nu/nu* mice bearing human colorectal carcinoma LS-174T xenografts. Biodistribution data were obtained at 1, 2, 3 and 4 d after intravenous injection of ^{86}Y-CHX-A"-DTPA-cetuximab. **(B)**. Dose-dependent receptor-meditated uptake of ^{86}Y-CHX-A"-DTPA-cetuximab in selected organs of female athymic (NCr) *nu/nu* mice bearing human colorectal carcinoma LS-174T 3 d after injection. All values are expressed as % ID/g. Data represent the mean value ± SEM from at least four determinations.

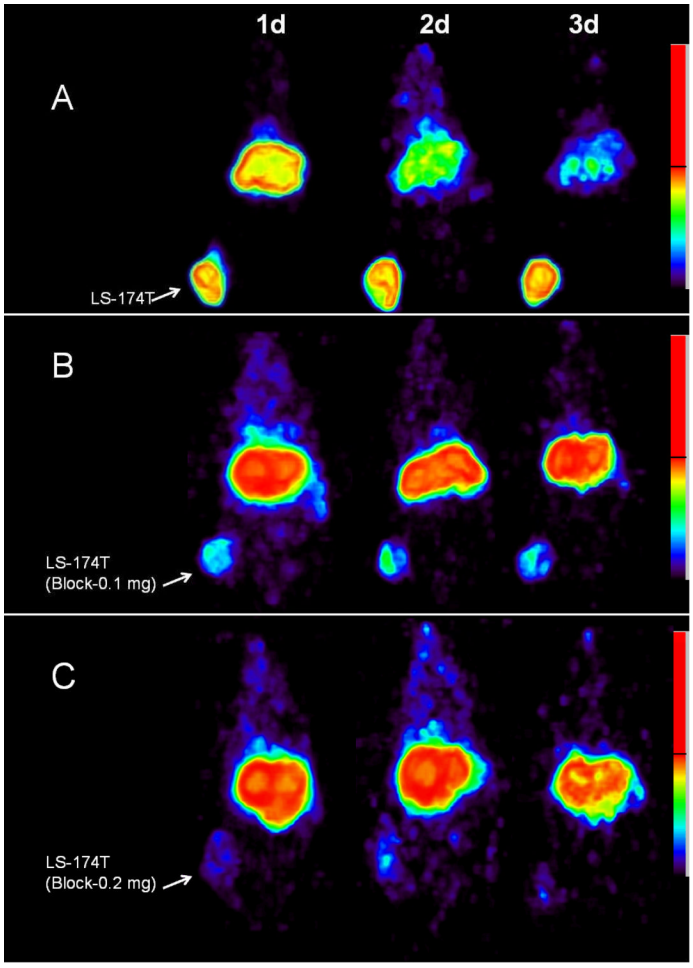

Figure 2.
(A) Representative reconstructed and processed maximum intensity projections of female athymic (NCr) *nu/nu* mice bearing human colorectal carcinoma LS-174T xenografts injected i.v. with 3.8–4.0 MBq of ^{86}Y-CHX-A”-DTPA-cetuximab (B) 3.8–4.0 MBq of ^{86}Y-CHX-A”-DTPA-cetuximab co-injected with 0.1 mg cetuximab and (C) 3.8–4.0 MBq of ^{86}Y-CHX-A”-DTPA-cetuximab co-injected with 0.2 mg cetuximab. The tumors are indicated with a white arrow.

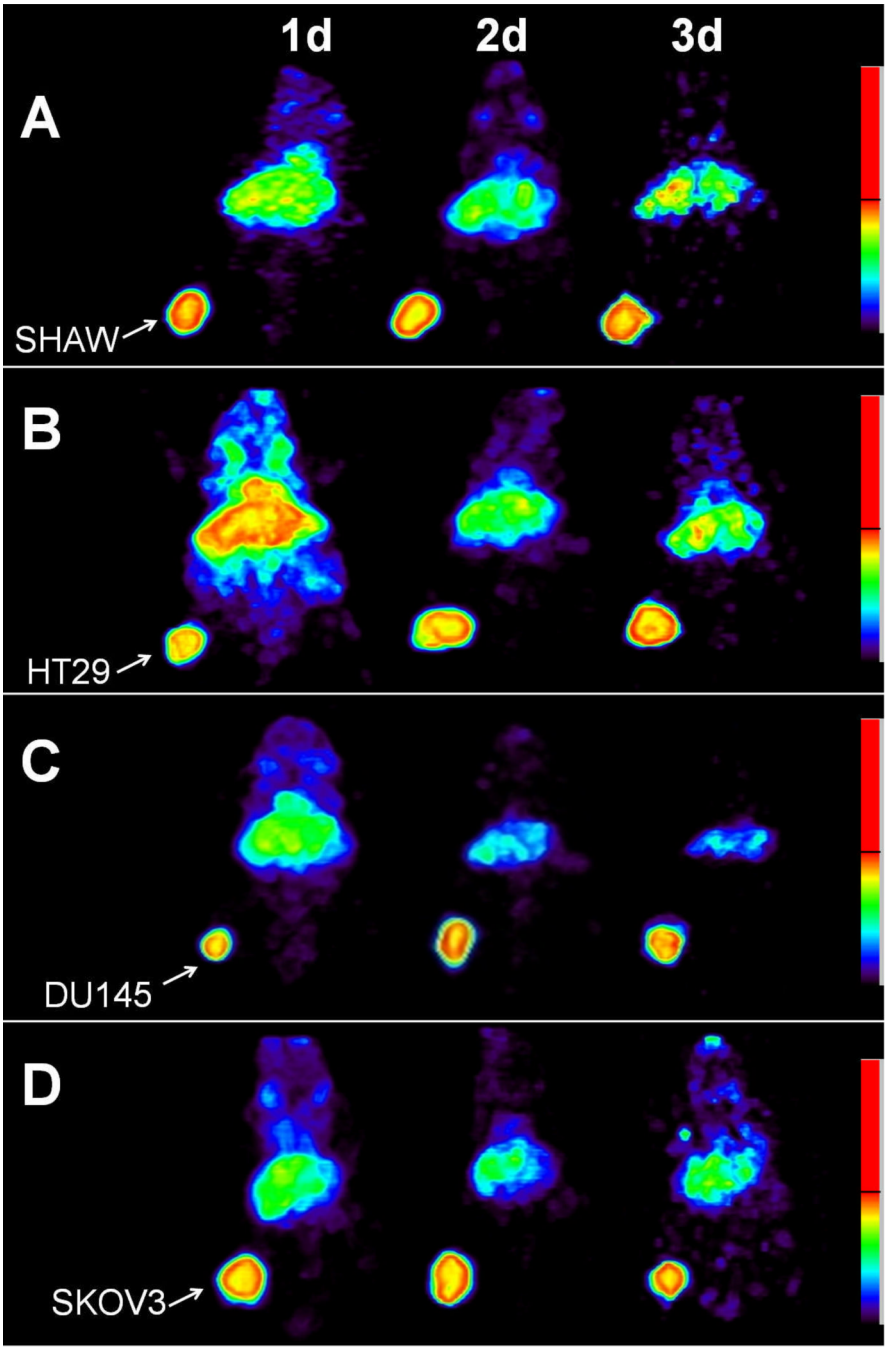

Figure 3.
Representative reconstructed and processed maximum intensity projections of female athymic (NCr) *nu/nu* mice bearing (A) human pancreatic carcinoma SHAW, (B) human colorectal carcinoma HT29, (C) human prostate carcinoma DU145 and (D) human ovarian carcinoma SKOV3 tumor xenografts injected i.v. with 3.8–4.0 MBq of ^{86}Y-CHX-A”-DTPA-cetuximab. The tumors are indicated with a white arrow.

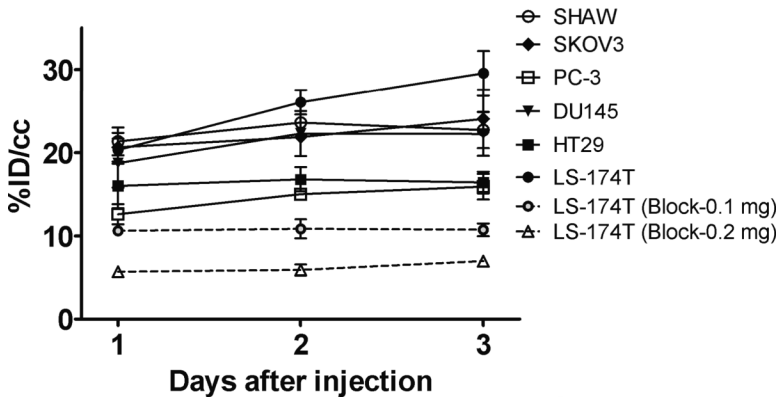

Figure 4.

Time-activity curve and uptake values of ^{86}Y-CHX-A”-DTPA-cetuximab in female athymic (NCr) *nu*/*nu* mice bearing HER1-expressing human tumor xenografts assessed through quantitative small animal PET imaging. All uptake values derived from PET studies are expressed as % ID/cc. Data represent the mean value ± SEM from at least three determinations.

Table 1

Pharmacokinetic characteristics of ^{86}Y-CHX-A”-DTPA-cetuximab. Pharmacokinetic characteristics of ^{86}Y-CHX-A”-DTPA-cetuximab injected intravenously via the tail vein of female athymic (NCr) *nu/nu* mice bearing tumor xenografts. Data represent the mean values from three to six determinations.

Tumor xenograft	$AUC_{[0\rightarrow3]}$ (%ID·d·cc^{-1})	$AUMC_{[0\rightarrow3]}$ (%ID·d^2·cc^{-1})
HT29	33.00 ± 1.85	66.20 ± 2.43
DU145	42.91 ± 5.20	87.35 ± 10.62
SKOV3	43.82 ± 1.64	91.47 ± 6.78
SHAW	43.60 ± 0.68	89.31 ± 2.62
PC-3	27.24 ± 2.33	59.54 ± 3.09
LS-174T	50.99 ± 1.17	106.60 ± 3.43
LS-174T (Block-0.1 mg)*	21.50 ± 1.77	43.07 ± 3.62
LS-174T (Block-0.2mg)*#	12.22 ± 0.86	25.08 ± 1.59

*The AUC and AUMC values of mice bearing LS-174T injected with ^{86}Y-CHX-A”-DTPA-cetuximab were significantly different ($p < 0.001$) than mice injected with ^{86}Y-CHX-A”-DTPA-cetuximab co-injected with 0.1 mg and 0.2 mg cetuximab to block the receptor.

#The AUC and AUMC values of mice bearing LS-174T co-injected with 0.1 mg cetuximab were significantly different ($p < 0.05$) than mice co-injected with 0.2 mg cetuximab to block the receptor.